

The role of dislocations as nonradiative recombination centers in InGaN quantum wells

Josh Abell^{a)} and T. D. Moustakas

Department of Electrical and Computer Engineering, Center for Photonics Research, Boston University, Boston, Massachusetts 02215, USA

(Received 10 November 2007; accepted 7 February 2008; published online 3 March 2008)

InGaN multiple quantum wells (MQWs) were grown on atomically smooth *c*-GaN templates and identical *c*-GaN templates etched to reveal hexagonal pits associated with screw dislocations. We found that the room temperature internal quantum efficiency of the MQWs grown on the etched *c*-GaN templates is a factor of 2 higher than that of the smooth QWs. This finding is accounted for by the fact that the QWs on the nonplanar surfaces are thinner than the *c*-plane QWs, and thus the carriers are prevented from reaching the dislocations due to the energy barrier around each defect.

© 2008 American Institute of Physics. [DOI: 10.1063/1.2889444]

InGaN quantum wells (QWs) are used as the active region of blue-green light-emitting diodes (LEDs). These materials and device structures are generally grown heteroepitaxially on the *c*-plane sapphire or SiC substrates. Due to large lattice and thermal mismatches between substrate and films, these materials have a high concentration of threading defects (edge, screw and mixed dislocations, and inversion domain boundaries) as well as planar defects (stacking faults) and point defects.¹ Furthermore, InGaN alloys tend to undergo both phase separation as well as long-range atomic ordering which give rise to potential fluctuations due to compositional inhomogeneities.^{2,3}

In spite of the high concentration of defects in the InGaN alloys, the internal quantum efficiency (IQE) of multiple QWs and LEDs based on such multiple QWs (MQWs) was found to be very high.⁴ A number of recent papers have addressed the origin of the high internal quantum efficiency in such QWs. For example, Chichibu *et al.* presented arguments that the high IQE is related to localization of excitons in indium-rich regions due to the compositional inhomogeneities.⁴ Other papers argue that threading dislocations are negatively charged and therefore prevent electrons from migrating toward them.^{5,6} Hangleiter *et al.* presented an alternative model to account for why the threading dislocations are not efficient nonradiative recombination centers.⁷ These authors have correlated the existence of V defects in metal-organic chemical-vapor deposition grown InGaN QWs with recombination processes of injected carriers. These V defects are hexagonal pits with (10–11) sidewalls terminating threading dislocations. The formation of these defects is attributed to the lower growth rate of the (10–11) facets.⁸ Specifically, Hangleiter *et al.* have observed that the QWs at the (10–11) facets are thinner than the QWs on the (0001) flat areas of the wafer and proposed that electron-hole pairs generated in the flat regions of the MQWs are prevented from recombining at dislocations due to energy barriers between the two types of QWs. In this paper, we investigated the role of dislocations as nonradiative recombination centers by growing InGaN MQWs on *c*-GaN templates which have been intentionally etched to reveal pits associated with screw dislocations.

A GaN template, 5 μm thick, was deposited by the hydride vapor phase epitaxy (HVPE) method on a 2 in. (0001) sapphire substrate. The template was then quartered and three of the quarters were etched in HCl gas flow in the same HVPE reactor at 650 °C at varying times and HCl flow rates. One quarter, sample A, was left unetched, sample B was etched for 25 min at 5 SCCM (SCCM denotes cubic centimeter per minute at STP) of HCl, sample C was etched for 40 min at 5 SCCM of HCl, and sample D was etched for 30 min at 10 SCCM of HCl.

The quarters were loaded into a molecular beam epitaxy (MBE) system for epitaxial growth of InGaN/GaN MQWs. First, 100 nm of GaN was grown at 800 °C under Ga-rich conditions to establish the epitaxial growth. The substrate temperature was then lowered to 670 °C to grow seven periods of InGaN/GaN QWs. The wells were 30 Å thick $\text{In}_{0.25}\text{Ga}_{0.75}\text{N}$ and the barriers were 35 Å thick GaN. All four samples were grown under identical conditions.

The templates and MQWs were then characterized by scanning electron microscopy (SEM) and photoluminescence (PL) using a 10 mW HeCd laser as the excitation source. The PL spectra were also measured as a function of temperature from 10 to 300 K. The IQE at room temperature of the InGaN MQWs was calculated by taking the ratio of the integrated PL intensity at room temperature divided by the integrated PL intensity at 10 K.⁴

Figure 1 shows the SEM surface morphology of sample B after etching. Etching with HCl under these conditions reveals a network of etch pits associated with screw threading dislocations.⁹ We have examined our etched GaN films by atomic force microscopy and found that the angle of the facets was approximately 45° off of the (0001) planes. Thus, these facets correspond to the (10–12) planes which are 43.2° off the *c* plane. The density of the pits from the data of Fig. 1 was found to be $\sim 4 \times 10^8 \text{ cm}^{-2}$. For samples C and D, which were etched more extensively, we found that the density of the pits is the same; however, their size increases with the degree of etching until they begin to coalesce. Additionally, MBE regrowth of the MQWs was conformal to the template surface.

Figure 2 shows the room temperature PL spectra of each sample. All four spectra have a main peak in the spectral region between 480 and 490 nm with full width at half maxi-

^{a)}Electronic mail: jbell@bu.edu.

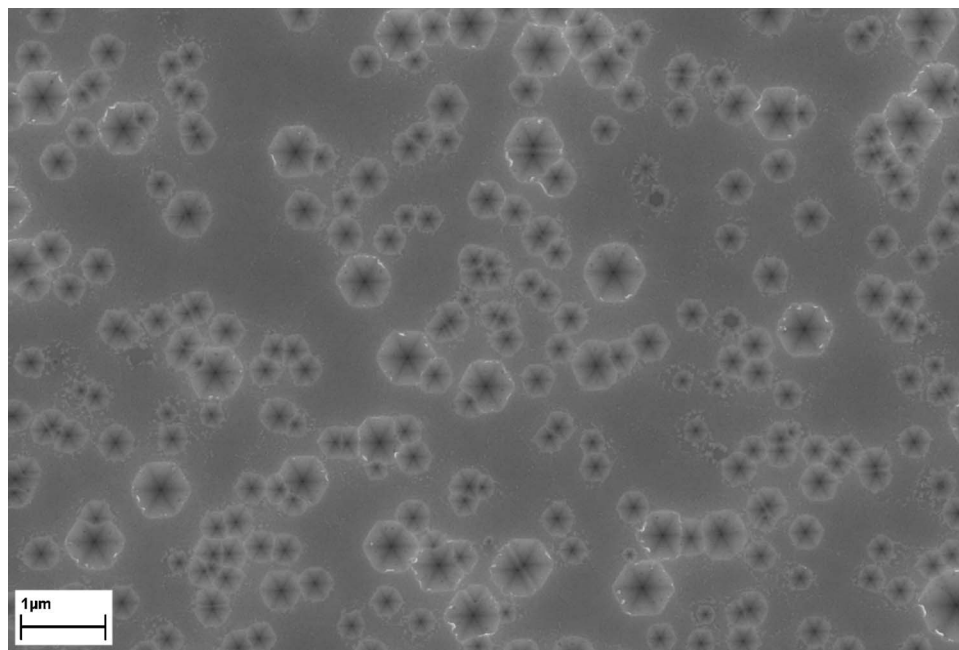


FIG. 1. SEM surface morphology of a HVPE-grown GaN template after etching at 600 °C for 25 min in 5 SCCM of HCl.

mum (FWHM) of approximately 50 nm. The etched samples have an additional peak in the spectral range of 420–430 nm with FWHM of approximately 22 nm. The intensity of this second peak increases with the degree of etching of the GaN template prior to the growth of the QWs. This result suggests that the origin of this peak is related to QWs on the inclined (10–12) planes.

To quantitatively account for the PL spectra of the MQWs, we show in Fig. 3 a schematic of the area around the (10–12) pit after the QW growth. From electron microscopy studies reported by our group,¹⁰ the MQWs on the (10–12) facets are thinner than those on the (0001) planes. There are two factors which account for this observation. First, the arriving fluxes of the Ga, In, and N beams are distributed over a larger area in the pits than the corresponding *c*-plane surface. Thus, we expect the thicknesses of the InGaN wells measured in the *c* direction on the (10–12) planes to be $d_v = d_{(0001)} \times \cos(43.2^\circ)$, where $d_{(0001)}$ is the thickness of the (0001) plane QW. Second, by taking into account the geometrical shape of the pits, the thickness of the (10–12) wells

in the confinement direction is $d_{(10-12)} = d_v \times \cos(43.2^\circ)$. Therefore, the thickness of the (10–12) wells is expected to be 0.53 times the thickness of the wells on the *c* plane. Because the QWs are thinner in the inclined (10–12) facets, emission from those QWs is expected to be blueshifted with respect to the (0001) QWs. Furthermore, the polarization vectors in the (10–12) QWs are no longer perpendicular to the well and so the piezoelectric fields are similarly reduced. This lessens the quantum confined Stark effect which leads to an even larger blueshift from the wells grown on the (0001) planes. Taking into account both the thicknesses of the QWs as well as the polarization effects, we calculated the emission energies by solving the Poisson and Schroedinger equations independently. The emissions for these MQWs are 439 and 492 nm for the (10–12) and (0001) wells, respectively, in approximate agreement with the observed PL spectra.

The IQE of the main peak in the PL spectra was determined by measuring the PL spectra as a function of temperature for all four samples. Figure 4 shows an Arrhenius plot of the integrated PL intensity $I(T)$ for sample A. The data were fitted using the following expression:

$$I(T) = \frac{I(0)}{1 + A_1 \exp\left(-\frac{E_{A_1}}{k_B T}\right) + A_2 \exp\left(-\frac{E_{A_2}}{k_B T}\right)}. \quad (1)$$

The two activation energies for nonradiative recombination processes, E_{A_1} and E_{A_2} , were found to be 13 and 79 meV,

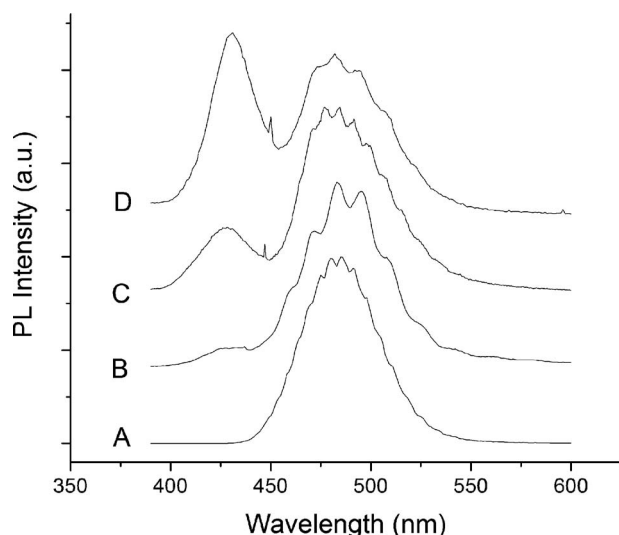


FIG. 2. The room temperature PL spectra for samples A, B, C, and D.

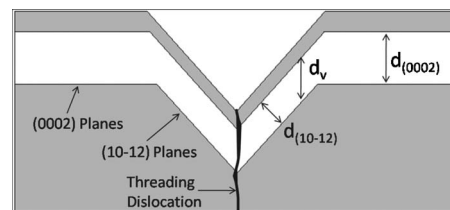


FIG. 3. Schematic of the area around the (10–12) pit after the QW growth. All relevant well thicknesses and growth planes are labeled.

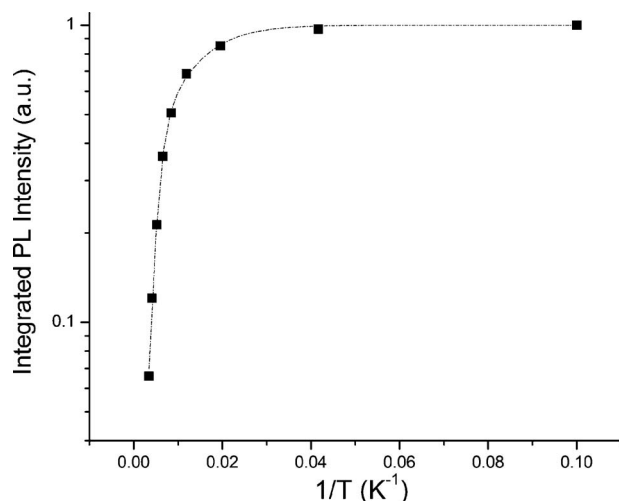


FIG. 4. Arrhenius plot of the integrated PL intensity $I(T)$ for sample A.

respectively, and correspond to two different mechanisms of PL quenching. The low temperature quenching mechanism of 13 meV is attributed to thermal delocalization of excitons from potential fluctuations arising from thickness variations in the wells or compositional inhomogeneities. The high temperature quenching mechanism of 79 meV is attributed to the lateral diffusion of carriers to dislocations where they recombine nonradiatively. Similar analysis was carried out for the etched samples B, C, and D and we found that the low temperature quenching mechanism is approximately the same as sample A, while the high temperature quenching has increased for the etched samples to approximately 95 meV. This result suggests that there is a larger barrier for nonradiative processes for the etched samples.

The IQE of sample A is 4.9%, consistent with reported values for c -plane $\text{In}_{0.25}\text{Ga}_{0.75}\text{NQWs}$ ⁴, while the IQE for the etched samples is approximately 10%. This result is consistent with the calculated barrier for nonradiative processes

discussed previously. This finding qualitatively agrees with the model proposed by Hangleiter *et al.*⁷ that the carriers from the (0001) MQWs have to overcome an energy barrier in order to migrate to dislocations where they can recombine nonradiatively.

In conclusion, we have demonstrated a suppression of nonradiative recombination in screw dislocations in InGaN MQWs by growing such structures on GaN templates which have previously been etched to reveal (10–12) pits associated with screw dislocations. Specifically, we found that the IQE of the MQWs grown on the etched c -GaN template is a factor of 2 higher than similar QWs grown on atomically smooth surfaces. This result was accounted for by the fact that the QWs on the (10–12) planes are significantly thinner than the c -plane QWs.

This work was supported partially by the Department of Energy (DE-FC26-04NT42275) and UNLV Research Foundation.

¹S. D. Lester, F. A. Ponce, M. G. Craford, and D. A. Steigerwald, *Appl. Phys. Lett.* **66**, 1249 (1995); F. A. Ponce and D. P. Bour, *Nature (London)* **386**, 351 (1997); S. Nakamura, *Science* **281**, 956 (1998).

²I. Ho and G. B. Stringfellow, *Appl. Phys. Lett.* **69**, 2701 (1996).

³D. Doppalapudi, S. N. Basu, K. F. Ludwig, Jr., and T. D. Moustakas, *J. Appl. Phys.* **84**, 1389 (1998).

⁴S. F. Chichibu, A. Uedono, T. Onuma, B. A. Haskell, A. Chakraborty, T. Koyama, P. T. Fini, S. Keller, S. P. DenBaars, J. S. Speck, U. K. Mishra, S. Nakamura, S. Yamaguchi, S. Kamiyama, H. Amano, I. Akasaki, J. Han, and T. Sota, *Nat. Mater.* **5**, 810 (2006).

⁵D. Cherns and C. G. Jiao, *Phys. Rev. Lett.* **87**, 205504 (2001).

⁶J. Cai and F. A. Ponce, *Phys. Status Solidi A* **192**, 407 (2002).

⁷A. Hangleiter, F. Hitzel, C. Netzel, D. Fuhrmann, U. Rossow, G. Ade, and P. Hinze, *Phys. Rev. Lett.* **95**, 127402 (2005).

⁸J. E. Northrup, L. T. Romano, and J. Neugebauer, *Appl. Phys. Lett.* **74**, 2319 (1999).

⁹T. Hino, S. Tomiya, T. Miyajima, K. Yanashima, S. Hashimoto, and M. Ikeda, *Appl. Phys. Lett.* **76**, 3421 (2000).

¹⁰J. C. Cabalu, C. Thomidis, I. Friel, T. D. Moustakas, and S. Riyopoulos, *J. Appl. Phys.* **99**, 064904 (2006).